Comparative Study on Structures and Energetics of NO_x, SO_x, and CO_x Adsorption on Alkaline-Earth-Metal Oxides

Elly J. Karlsen,[†] Martin A. Nygren,[‡] and Lars G. M. Pettersson*[,‡]

Oil and Energy Research Centre Porsgrunn, Section for Hydrocarbon Processes and Catalysis, Norsk Hydro ASA, N-3907 Porsgrunn, Norway, and FYSIKUM, AlbaNova, Stockholm University, S-106 91 Stockholm, Sweden

Received: March 16, 2003; In Final Form: May 15, 2003

Embedded cluster models of the (001) terrace site have been used to determine adsorption structures and energetics for NO_x (NO_2, NO_3), SO_x (SO_2, SO_3), as well as for CO_2 on the entire sequence (MgO−BaO) of alkaline-earth-metal oxides. The calculations have been performed at the gradient-corrected density functional level. The oxidation of NO, NO_2, SO_2, and CO using surface peroxo species is also considered with the aim of contributing to the understanding of car emission control catalysts based on the NO_x storage and reduction concept. For all substrates, the stability of the formed surface species is in the order $NO_2^- \approx CO_3^{2-} < NO_3^- < SO_4^{2-}$. Between substrates the stability of the adsorbates is determined by the substrate basicity, which in turn is regulated by the lattice parameter. The resulting order is MgO < CaO < SrO < BaO. Several different bonding modes and structures are found, which differ in terms of degree of charge transfer from the substrate and how the resulting charge deficiency in the substrate is distributed among the surface ions.

1. Introduction

There has been a recent surge of interest in the interaction of nitrogen oxides (NO_x) with alkaline-earth-metal oxides, in particular BaO. This is due to the recent development of NO_x storage catalysts for posttreatment of car exhaust gases under lean-burn conditions, i.e. in oxygen excess. In a traditional transition-metal-based, three-way car emission control catalyst, the oxidation of CO and remaining hydrocarbon fragments is performed simultaneously with the reduction of NO_x. For these catalysts to operate properly, the engine must be run with a stoichiometric fuel-to-air ratio, resulting in incomplete combustion and part of the energy-release occurring over the catalyst.[1] The lean-burn engine performs a complete combustion in the working step, which leads to lower fuel consumption, i.e. better economy, and thus reduced CO_2 emission as well as production of NO_x. The abatement treatment can now be focused on reduction of NO_x rather than also oxidizing CO and hydrocarbon fragments. Catalysts that support a storage capacity for nitrogen oxides have in this context attracted considerable attention. Since reduction of nitrogen oxides is difficult in an oxygen-rich environment, the NO_x is instead stored and the storage component regenerated periodically through a transient step with rich fuel mixture using the nitrogen oxides as oxidants. On the basis of these principles, a catalyst has been developed containing supported precious metals and barium oxide as storage component.[2] The exhaust gas contains CO_2, H_2O, O_2, and NO_x as main reactive components, and the BaO surface must thus be considered to be in a dynamic competition between the formation of carbonates, hydroxides, peroxides, and the desired stored nitrites and nitrates. Sulfur adsorbs irreversibly under the working conditions of the storage catalyst and thus acts as a poison. Due to the importance of these processes, there have recently been several experimental as well as theoretical studies on the interaction of both NO_x and SO_x with BaO and MgO, where the latter may be regarded as a simplified model system.

There seems at present to be two major mechanistic proposals for how the uptake of nitrate on the surface occurs. Broqvist et al.[3] investigated NO_2 adsorption on BaO and found a cooperative effect in a mechanism where the initial adsorption occurred on a surface anion. The adsorbed nitrite would subsequently transfer to the cation to leave room for a second NO_2 on the same BaO unit. Interconversion to a nitrate and removal of NO combined with a third NO_2 adsorbing to form a second nitrate provides a plausible interpretation of the experimentally observed stoichiometry of one NO released per two surface NO_3 formed.[4] This interpretation was later supported by Hess and Lunsford,[5] who observed initial nitrite formation followed by conversion to nitrate upon exposure of BaO to NO_2 in the absence of oxygen. However, inclusion of 20% O_2 in the gas flow at 400 °C lead to enhanced and direct nitrate formation without the nitrite step. This would be indicative of the second proposed mechanism, which is assumed to involve direct reaction with surface peroxides, and indeed, formation of peroxides was observed in the initial phase of the reaction.[5] At lower temperatures both nitrite and direct nitrate formation were observed also in the presence of O_2.

The cooperative effects upon adsorption of NO_x on MgO(001) were demonstrated and investigated by Schneider and coworkers.[6] Since the relevant NO_x species can form strongly interacting Lewis acid−base pairs when adsorbed on nearby sites, while the isolated adsorbates on MgO(001) are only physisorbed, the cooperative effects were found to be dramatic. For a pair of NO_2 molecules an additional stabilization of 15 kcal/mol was obtained. It was suggested that for BaO(001) an even larger effect should be expected. However, with consideration of the proposed thermodynamic cycle, i.e., charge transfer in the gas phase to create the Lewis acid−base pair, subsequent isolated adsorption followed by moving the adsor-

* Author to whom correspondence should be addressed. E-mail: lgm@physto.se.
[†] Norsk Hydro ASA.
[‡] Stockholm University.

10.1021/jp0346716 CCC: $25.00
Published on Web 07/04/2003

bates to adjacent positions, the electrostatic stabilization effect could be expected to be strongly reduced on BaO. This is due to its substantially larger lattice parameter, 5.52 Å compared to 4.21 Å for MgO.[7] In accordance with this reasoning, the cooperative effect found by Broqvist et al. for an NO_2 pair on BaO was only 2 kcal/mol[3]. If one furthermore considers the reduction of the electrostatic stabilization that can be expected for a nonfully periodic adsorbed overlayer (as would result from competing adsorption from the exhaust gas-mixture), as well as from a structurally defective substrate, the importance of the cooperative effect may well be reduced compared to what was found for MgO.

From the above it is clear that several different processes should be possible and could be operative under different conditions for different substrates; adsorption and interaction of all the involved species must furthermore be considered. It has, for example, been observed that NO_x storage decreases with the CO_2 partial pressure in the feed gas.[8,9] Moreover, Rodrigues et al.[10] have shown that CO_2 and NO_2 are competing for the same trapping barium site. Sulfur is furthermore a trace contaminant in fuels, and when the storage component is exposed to SO_x (SO_2 and SO_3) the formed stable barium sulfites and sulfates compete with and inhibit nitrate formation. So far, the mechanism for SO_x adsorption has been investigated only for MgO and CaO.[11,12] We complete the picture of SO_x interaction by including both SrO and BaO as substrates in the present work.

In the experimental investigations performed so far, SrO has mainly been neglected. However, a recent study of the NSR process by Pyng-Hyun et al. did include CaO, SrO, as well as BaO.[13] The $Pt/SrO/Al_2O_3$ catalyst was found to be of efficiency similar to that of $Pt/BaO/Al_2O_3$, while both showed substantially higher efficiency than for the combination with CaO. To elucidate the specific factors determining the efficiency of the NSR concept for the alkaline-earth oxides it is a great advantage to include the entire sequence MgO−BaO in the investigation. In the present work we have focused on the adsorption structure and energetics for single-adsorbate NO_x, CO_x, and SO_x on the alkaline-earth-metal oxides using embedded cluster models of the substrate. The results are relevant for discussing the initial steps in a cooperative adsorption as well as of direct relevance to mechanisms involving reaction with surface peroxo species, which may be formed, e.g., on BaO in oxygen excess. Possible mechanisms for the different substrates, including surface transport, will be discussed in a forthcoming paper.[14]

The adsorption properties can be correlated with the basicity of the substrate. In the sequence MgO to BaO of alkaline-earth-metal oxides the lattice constant increases strongly, which means that the electrostatic stabilization of the ionic charge separation is stepwise reduced. At the surface, the electron-donating property (or the basicity) increases for increasing lattice parameter.[12,15−17] By studying this sequence of related substrates we can draw conclusions on how the electron-donating properties of the materials influence the chemistry. Another important aspect is that as errors at a certain level of theory tend to be systematical, comparisons between several cases will be more reliable than each calculation in isolation.

2. Computational Details

Embedded cluster models as representation of the surface is the key approximation made in the present work. The embedding is constituted of Embedding Ab Initio Model Potentials (EAIMP) at nearby sites and an infinite point charge array to describe the long-range electrostatic contribution.

The basis sets employed for the adsorbates have been those of Dunning[18] with a generally contracted core for carbon, oxygen, and nitrogen, whereas the sulfur basis was the D95V.[19] To give a good description of the oxygen anion, we used the basis set of Dunning[18] extended with an extra, diffuse *s*-function where the diffuse *p* and *d*-functions have been reoptimized.[20] The magnesium cation has been described by the MIDI-4 basis.[21] For Ca, Sr, and Ba, the core electrons were described by effective core potentials (ECP) and only the outermost electrons were explicitly treated in the calculations. Both the core potentials and the basis sets were taken from Hay and Wadt.[22] The core potentials used here replace only the inner core electrons and treat the 10 outermost electrons explicitly as valence electrons ($[\text{core}]ns^2np^6(n+1)s^2$). Embedding model potentials have been used for ions out to a distance of 11.3 Bohr from any cluster ion. These potentials provide an approximate description of short-range Coulomb, exchange, and orthogonality interactions, as well as a representation of relativistic effects, based on the frozen ions.[23,24]

Long-range electrostatic contributions are included by computing the integrals over the Ewald sum[25] for the infinite point charge array using the method of Parry[26,27] for surfaces. The Ewald summation code was originally written by Nygren and included in the model potential code ECPAIMP written by Seijo and Pettersson.[28] In the present work we employ the implementation by Nygren and Hall[29] of this embedding technique in the Gaussian98 package.[30]

In the search for the energy minima for adsorption on the anion, the position and internal geometries of the adsorbate as well as the distance between the central oxygen and second layer of the surface were optimized. The surface cluster model consisted of an embedded Me_5O_5 for CO_x and SO_x adsorption. Upon NO_2 and NO_3 adsorption, it has been shown in a previous theoretical study that the spin is delocalized over the neighboring surface oxygen sites.[3] To describe this type of interaction, we have employed a larger cluster model (Me_9O_9) where these oxygen sites are included as well. For adsorption on surface cations a Me_8O_8 cluster is used. Here the distances between the second layer and the central surface cation and the anion were optimized for the central Me_4O_4 surface unit. All calculations have been performed at the gradient-corrected DFT level using the B3LYP functional.

3. Results and Discussion

The results in the present work are divided and discussed in three parts. The first section is devoted to NO_x adsorption. The adsorption of CO_x and SO_x are addressed in the two last sections.

NO_x Adsorption. The adsorption of NO_x species on the ionic alkaline-earth-metal oxide surfaces is governed by several factors. In general there is a charge transfer from the surface to the adsorbate, which is governed by the basicity of the surface anionic sites. This is in turn determined by the lattice parameter; i.e., the smaller the lattice parameter the larger the internal Madelung stabilization and the smaller the charge transfer. The electrostatic stabilization of the adsorbate depends on the ability of the adsorbate to interact favorably with the charge distribution in the lattice. In summary, we find several different adsorption possibilities where the balance between them depends on the particular case considered.

Previous work on BaO by Broquist et al. has shown that NO_2 may adsorb both on single surface oxygen and cation sites, where the highest adsorption energy was obtained for the anion site.[3] For MgO, Schneider and co-workers have shown that single NO_3 and NO_2 preferentially adsorb on cation-pair sites.[6]

TABLE 1: NO_2 Adsorption on a Surface Oxygen Site[a]

substrate	$r(NO_2-O\_s)$	$r(NO)$	$\alpha(ONO)$	$q(NO_2)$	$sd(NO_2)$	E1	E2
MgO	2.75	1.20	131.6	−0.05	0.87	−3.8	−42.3
CaO	2.15	1.22	126.5	−0.32	0.60	−16.7	−28.0
SrO	2.14	1.23	124.1	−0.42	0.53	−21.5	−21.5
BaO	2.18	1.23	122.8	−0.45	0.47	−25.9	−17.6

[a] The bond distances are given in Å, angles in degrees, and energies in kcal/mol. $r(NO_2-O\_s)$ denotes the NO_2 distance to the surface oxygen and $q(NO_2)$ is the Mulliken charge on the adsorbed NO_2 unit. $sd(NO_2)$ is the spin-density on the NO_2 unit. See Figure 1 for the geometrical orientation on the surface. E1 denotes the reaction energy for direct adsorption of NO_2 on the surface oxygen site, whereas E2 is the calculated reaction energy for NO oxidation to NO_2 over a surface peroxide site.

TABLE 2: NO_2 Adsorption on a Surface Cation-Pair Site[a]

substrate	$r(NO_2\text{-surf})$	$r(NO)$	$\alpha(ONO)$	$q(NO_2)$	$sd(NO_2)$	energy
MgO	2.44	1.20	130.9	0.07	0.84	−9.0
CaO	2.52	1.24	118.5	−0.54	0.40	−18.3
SrO	2.66	1.25	116.0	−0.73	0.05	−24.8
BaO	2.86	1.26	115.8	−0.76	0.02	−31.0

[a] The bond distances are given in Å, angles in degrees, and energies in kcal/mol. $r(NO_2\text{-surf})$ denotes the NO_2 distance to the surface oxygen, and $q(NO_2)$ is the Mulliken charge on the adsorbed NO_2 unit. $sd(NO_2)$ is the spin-density on the NO_2 unit. See Figure 2 for the orientation of NO_2 on the surface.

On the basis of these observations, we have investigated the adsorption of NO_x on the most favorable adsorption sites such as the surface oxygen anion as well as the cation-pair sites, for the entire sequence of alkaline-earth-metal oxides in order to investigate the fundamental factors determining these interactions. Since BaO is the technologically most interesting substrate, we have for this case also investigated adsorption of NO_3 at a single surface cation site.

NO_2 Adsorption. The results (see Tables 1 and 2) show that the adsorption energies in the case of MgO−BaO for the cation-pair and anion sites are very similar. The electronic structure of gas-phase NO_2 is $^2A_1$ with an electron affinity of 2.27 eV;[31] electron transfer from the substrate thus results in a reduced spin-density on the adsorbed NO_2 and a concomitant increase in the substrate. The highest occupied states in the substrate electronic structure, from which the charge transfer occurs, contain mostly contributions from the oxygen 2*p* states. How the resulting spin-density is distributed in the substrate is one of the considerations in analyzing the resulting bonding. For the oxygen anion site, there is in general a smaller charge transfer and the spin density is localized on both the adsorbate and the central surface oxygen anion, while for the cation-pair site the resulting spin density is delocalized over the surface oxygens. For MgO and CaO there is only a partial charge-transfer resulting in similar spin density on the adsorbate and in the surface, while for SrO and BaO the spin-density on the adsorbate is very small, indicating a near-complete transfer of one electron to the NO_2 at the cation-pair site. The calculated energies show that for all substrates the cation-pair site is slightly more favorable than the oxygen anion site, in agreement with what was found by Schneider et al. for MgO.[6]

For adsorption on an oxygen anion, the charge density is shared by the adsorbate and the central surface oxygen anion, thus indicating only a partial electron transfer from the surface oxygen site to NO_2. Along the sequence MgO−BaO, the adsorption energy reveals the expected trend, that is, an adsorption energy that follows the increasing lattice parameter: MgO < CaO < SrO < BaO. NO_2 adsorption on MgO is weak (3.8 kcal/mol) with no charge transfer from the surface. This is also reflected in the internal geometry of the adsorbed NO_2, which is hardly changed compared to the gas-phase structure ($r(NO)$ = 1.19 Å, $\alpha(ONO)$ = 134.4°). For CaO−BaO the perturbation of the adsorbed NO_2 increases along this series, where the $r(NO)$ bond distance becomes more elongated and the angle decreases. For the oxygen anion site, the adsorbate distance to the surface is largest for the more weakly interacting MgO, while CaO, SrO, and BaO show rather similar NO_2 to surface distances with small differences. The trends in internal geometry and charge transfer, i.e., the correlation with the lattice parameter, show the expected increased charge transfer as the lattice parameter increases along the series.

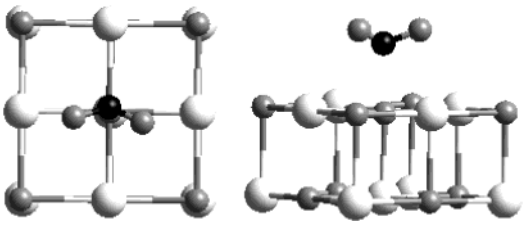

Figure 1. NO_2 adsorption on surface anion site. The metal atoms are given in white, oxygen atoms in gray, and nitrogen in black.

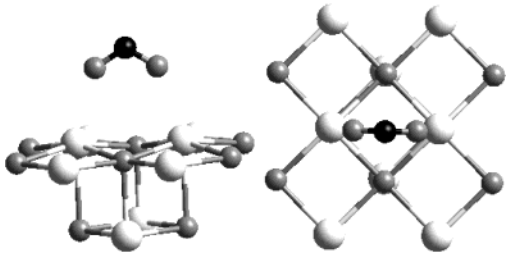

Figure 2. NO_2 adsorption on surface cation-pair site. The metal atoms are given in white, oxygen atoms in gray, and nitrogen in black.

For the cation-pair site the perturbation of the internal adsorbate geometry is larger and the structure approaches that of gas-phase NO_2^- ($r(NO)$=1.26 Å, $\alpha(ONO)$ = 115.9°) in accordance with the near-complete charge transfer in the cases of adsorption on SrO and BaO. There is no resulting spin-density on the cations, indicating that the charge-transfer is from the surface oxygens as expected. The difference between the substrates lies in the distribution of the resulting spin-density on the surface anions. For MgO the spin-density (0.14) in the substrate is entirely localized on the two surface oxygens in the local Me_4O_4 subunit, while for CaO, SrO, and BaO even larger values are obtained for the local anions (0.4−0.5), but here the surrounding anions also contribute of the order of 0.2−0.5 following the increase in lattice parameter.

In contrast to the case for the oxygen site, the NO_2 distance above the surface at the cation-pair site follows a trend along the sequence, where it increases along MgO to BaO. This distance reflects the increasing size of the cations in the surface, but not the surface relaxation where the geometry optimization reveals a movement of the cations out of the surface, which is almost the same (+0.3 Å) for CaO, SrO, and BaO. This is somewhat surprising since one would expect an increasing mobility with increasing lattice constant. The movement of the surface oxygen into the bulk (CaO: −0.005 Å, SrO: −0.03 Å, BaO: −0.04 Å) follows more the trend of the lattice constants.

The orientations of the adsorbate on the surface in the two situations are given in Figures 1 and 2. Only the geometries giving the lowest adsorption energy are reported here. For all oxides, the orientation of NO_2 is such that the oxygen atoms are directed between the nearest surface cations. By comparing

the obtained adsorption energy and geometry with periodic slab calculations on BaO by Broqvist et al.[3] there is a discrepancy both in adsorption energy and geometry. Broqvist et al. report an adsorption energy almost 30% lower than the one reported in the present work. Moreover, they calculate a larger NO_2 distance to the surface, in addition to a different orientation of the NO_2 adsorbate on the surface. This discrepancy is partly related to the fact that none of the surface atoms in the periodic slab calculations were relaxed during the geometry optimization. A test calculation in the present work, where the central surface oxygen was not included in the optimization, shows a reduction of the adsorption energy by about 5 kcal/mol. Moreover, in the periodic slab calculation, interactions between the adsorbed NO_2 could be present, which may result in destabilization of the adsorbed NO_2 on the surface. This is not taken into account in the embedded cluster model with only one adsorbate present. A comparison of our embedded cluster adsorption energy f*or* NO_2 on MgO (3.8 kcal/mol) with the periodic slab calculation of Schneider et al.[6] (4.3 kcal/mol) shows good agreement, however, which indicates that the remaining discrepancy is not due to the different surface models applied.

The type of interaction, on the other hand, between the adsorbate and the surface oxygen anion turns out to be the same for BaO using the embedded cluster and periodic slab calculations: NO_2 is found to be chemisorbed, with a partial charge transfer from the surface to the adsorbate, resulting in a perturbation of the internal geometry of NO_2. Adsorption on the cation-pair site shows an increased delocalization of the spin on the surface along the sequence, which implies that the adsorbate becomes more chemisorbed. Schneider et al. have considered this adsorption mode for MgO in a periodic slab calculation.[6] They obtain an adsorption energy of 10.5 kcal/mol for NO_2 on the cation-pair site, which is in good agreement with our result (9 kcal/mol), which is further indication that the result of Broqvist et al. is an underestimate of the interaction. The picture of a molecularly physisorbed NO_2 in the work in reference 6 is the same as that obtained in the present work. In the present study, the Mulliken population analysis reveals spin density only on the adsorbate in the interaction with MgO in accordance with the larger stabilization of the charges on this substrate and consequently smaller charge transfer to the adsorbate.

NO_2 has been demonstrated to form by oxidation of NO over the Pt catalyst in the step with lean mixture.[4,32] However, the formation of NO_2 from the reaction of NO with surface peroxide could also be a possible route in the NO_x storage process. The reaction energy for this process is here calculated to be 42.3, 28.0, 21,5, and 17.6 kcal/mol for MgO, CaO, SrO, and BaO, respectively. This indicates that if surface peroxides are present, this route to the formation of NO_2 from NO is energetically possible. These reaction energies reflect, in addition to stabilization of adsorbed nitrite, the relative stabilization of surface peroxide. In previous work, the peroxide stabilization energy was calculated to 34.6, 61.8, 73.1, and 81.4 kcal/mol for MgO, CaO, SrO, and BaO, respectively.[16] Thus, the relatively large binding energy of atomic oxygen on BaO results in a lower surface nitrite formation energy compared to direct adsorption of NO_2. However, the overall reaction, i.e., oxidation of NO over peroxide leading to adsorbed NO_2, is exothermic. Oxidation of NO on MgO and CaO by surface peroxide to NO_2(g) is calculated to be exothermic by 38.5 and 11.3 kcal/mol, respectively. For SrO, this reaction is thermoneutral and for BaO, endothermic by 8.3 kcal/mol. Thus, once NO is oxidized by surface peroxide, NO_2 remains adsorbed on all the substrates.

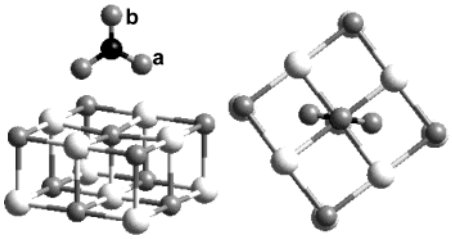

Figure 3. NO_3 adsorption on surface anion site. The metal atoms are given in white, oxygen atoms in gray, and nitrogen in black.

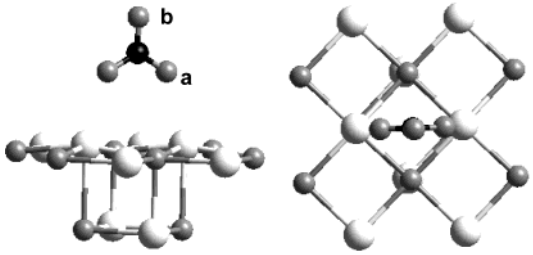

Figure 4. NO_3 adsorption on surface cation-pair site. The metal atoms are given in white, oxygen atoms in gray, and nitrogen in black.

As previously mentioned, the surface peroxide stability is lowest for MgO and CaO. In fact the MgO_2 and CaO_2 bulk peroxides are thermodynamically unstable.[33] If surface peroxides are formed from oxygen spillover from the noble metal particles (e.g., Pt), the peroxide stabilization energy on the metal oxide must be large enough to overcome the oxygen adsorption energy on, for example, Pt. With an adsorption energy of about 48 kcal/mol[32] for Pt particles, surface peroxide formation on at least MgO, through such a process is not likely. Oxidation of NO and NO_2 will occur over the Pt particles for all substrates. For SrO and BaO it seems likely that also surface peroxides could contribute to this oxidation process. The relative importance of NO and NO_2 oxidation over Pt vs oxidation over the surface peroxide will be considered in future work.

NO_3 Adsorption. All adsorption energies reported in this section are calculated with respect to the substrate and NO_3 in the gas phase. However, one should keep in mind that NO_3 is unstable in the gas phase by 9.1 kcal/mol toward $NO_2 + {}^1/_2O_2$,[34] and this energy should thus be added to the calculated adsorption energies when considering the lowest-energy desorption channel.

In contrast to NO_2, for which only minor differences in the adsorption energies were obtained for the two sites considered, the differences are much larger for NO_3. The cation-pair site is the most favorable adsorption site among those considered with an adsorption energy about 10 kcal/mol higher than that for the surface anion site.[3] The large adsorption energy of NO_3 compared to NO_2 is due to the substantially higher electron affinity of NO_3 (3.91 eV).[35] This can be seen when comparing the Mulliken charges for NO_3 and NO_2. The approximately NO_3^--like adsorbate binds strongly to the surface. Adsorption on the cation-pair site shows an increasing unpaired spin-density on the surface anions along the sequence, where for BaO the charge transfer from the surface is almost complete, resulting in a zero spin density on the adsorbate. The increasing charge transfer from the surface to the adsorbate along the sequence of metal oxides is further reflected in the adsorbate internal geometry, where one has an increasing perturbation of the internal geometry compared to the gas-phase structure (r(NO) = 1.23, α(ONO) = 120°).

The orientations of the NO_3 adsorbed on the surface oxygen and cation-pair sites are depicted in Figures 3 and 4. Again,

TABLE 3: NO_3 Adsorption on a Surface Oxygen Site[a]

substrate	r(N−O_s)	r(NO_a)	r(NO_b)	α(O_aNO_a)	α(O_aNO_b)	q(NO_3)	sd(NO_3)	E1	E2
MgO	2.94	1.23	1.22	115.5	125.5	−0.39	0.44	−19.9(−10.8)	−35.1
CaO	2.96	1.25	1.22	118.1	123.7	−0.62	0.23	−40.2(−31.1)	−28.1
SrO	3.09	1.28	1.23	119.1	120.5	−0.82	0.06	−47.7(−38.6)	−24.4
BaO	3.25	1.28	1.23	119.1	120.4	−1.29	0.03	−56.8(−47.7)	−25.2

[a]The bond distances are given in Å, angles in degrees, and energies in kcal/mol. r(N−O_surf) denotes the nitrogen distance to the surface oxygen, and q(NO_3) is the Mulliken charge on the adsorbed NO_3 unit. sd(NO_3) is the spin-density on the NO_3 Unit. See Figure 3 for labels and geometrical orientation of NO_3 on the surface. E1 denotes the reaction energy for direct adsorption of NO_3 on a surface oxygen site, whereas E2 is the calculated reaction energy for NO_2 oxidation to NO_3 over a surface peroxide site. The energy values given in parentheses are relative to NO_2 and $^1/_2O_2$, where the experimental value of ΔH_{298K} is used for the $NO_2 + {}^1/_2O_2 \rightarrow NO_3$.[34]

TABLE 4: NO_3 Adsorption on a Surface Cation-Pair Site[a]

substrate	r(NO_3-surf)	r(NO_a)	r(NO_b)	α(O_aNO_a)	α(O_aNO_b)	q(NO_3)	sd(NO_3)	energy
MgO	2.20	1.28	1.23	119.9	118.1	−0.41	0.27	−21.3 (−12.2)
CaO	2.46	1.27	1.23	118.8	120.6	−0.73	0.02	−47.9(−38.8)
SrO	2.64	1.27	1.23	118.7	120.6	−0.84	0.01	−58.4(−49.3)
BaO	2.83	1.27	1.23	118.6	120.7	−0.86	0.00	−66.5(−57.4)

[a] The bond distances are given in Å, angles in degrees, and energies in kcal/mol. r(NO_3-surf) denotes the nitrogen distance to the surface oxygen, and q(NO_3) is the Mulliken charge on the adsorbed NO_3 unit. sd(NO_3) is the spin-density on the NO_3 unit. See Figure 4 for labels and geometrical orientation of NO_3 on the surface.

the adsorbate surface distance increases along the sequence for both adsorption sites, while the adsorption energy increases.

The present results have been obtained using embedded cluster models with a single adsorbate taken explicitly into consideration and are thus strictly applicable in the low-coverage regime. High surface coverage could result in destabilization of the adsorbed species as demonstrated for the case of removal of peroxo species through reaction with N_2O on BaO.[36] We suggest however, that the cation-pair site could be important in the NO_x storage process and should therefore be taken into account when considering this process. Adsorption of NO_3 on a single cation site on BaO results in an adsorption energy (58.1 kcal/mol) very close to that of the oxygen anion site, but still less than the cation-pair site. Comparison of our embedded cluster (low-coverage) results for NO_2 adsorption on MgO(001) with those from the periodic (high-coverage) results of Schneider et al.[6] gives no indication of a strong influence of adsorbate−adsorbate interactions. However, considering that the energy difference between the most stable cation-pair site and the single anion or cation site is of the order of 10 kcal/mol, it is entirely possible that coadsorbates (hydroxyl, carbonates, etc.) could modify this balance and allow for adsorption also at these alternative sites. For the initial adsorption of a formed NO_3 unit, however, our results strongly indicate the cation-pair site to be the energetically most favored.

If nitrates ionically bound to the surface in the fashion described above constitute the dominating active species in the NO_x storage catalyst, the questions of where the NO_3 units are formed and how they are transported out over the surface become critical. If surface peroxide species are present, nitrate can be formed by a direct reaction between NO_2 and O_2^{2-}, where the reaction energies for MgO, CaO, SrO, and BaO are 35.1, 28.1, 24.4, and 25.2 kcal/mol, respectively. Again, these reaction energies also reflect the relative stability of the surface peroxide, which is least stable for MgO. As a consequence, the oxidation of NO_2 on MgO by surface peroxide to NO_3(g) is calculated to be exothermic by 15.2 kcal/mol. For CaO, SrO, and BaO, this reaction is endothermic by 12.0, 23.3, and 31.6 kcal/mol, respectively, but since the adsorption energy is also increasing the resulting reaction energies become nearly constant. Thus, once NO_2 is oxidized by surface peroxide, NO_3 remains adsorbed on all these substrates. However, as mentioned previously, oxidation of NO_2 over surface peroxides may be ruled out for MgO and CaO due to the instability of the corresponding bulk peroxides.[33]

As diffusion of atomically adsorbed oxygen cannot be expected to occur on the BaO surface,[16] this requires that a large enough quantity of peroxide species be generated at the surface for this mechanism to be contributing. In the presence of oxygen under the working conditions of the NO_x-storage catalyst, this can be expected to be the case; according to the phase-diagram for $(BaO + O_2)/BaO_2$, a large amount of peroxide can be expected to form.[37,38]

In the absence of surface peroxides, the nitrite-to-nitrate cooperative internal conversion mechanism could be active as also observed by Hess and Lunsford. In particular for SrO and BaO the bonding to the substrate is strong enough that the generated nitrate species would remain bound to the surface under the relevant conditions. For either scenario for the nitrate formation, diffusion of nitrates over the surface is likely to be involved, in particular in the regeneration step where dissociation of nitrate to the supported precious metal is believed to be involved. Possible mechanisms for nitrate diffusion are currently under investigation.[39]

Creation of Carbonate and Sulfate Ions at the Surface. Ions such as sulfates and carbonates can be formed by creation of a covalent bond between a surface oxygen anion and a gas-phase molecule in a direct adsorption mechanism. Surface carbonate or sulfate species formed like this will be anchored into the surface through one of the oxygens. Experimentally, it has been observed that carbonates and sulfates might be formed either in the bulk or at the surface. Previous theoretical works have focused on SO_x and CO_x adsorption on MgO and CaO.[11,12] For both MgO and CaO, the gas-phase CO_2, SO_2, and SO_3 were found to be anchored through C or S to the surface oxygen. This is also the result of the present work. The bonding mechanism seems to be general with the same type of coordination obtained also for SrO and BaO. A second possibility to consider is oxidation of CO and SO_2 species through reaction with peroxide species.

CO_2 Adsorption. For CO_2 adsorption, the oxygens in the adsorbed CO_2 are oriented upward from the surface for CaO−BaO (see Figure 5). For MgO, CO_2 is only physisorbed at the investigated terrace sites with a computed binding energy of only 3.5 kcal/mol. This is also reflected in the geometry of the adsorbate, which is only slightly perturbed compared to the gas-

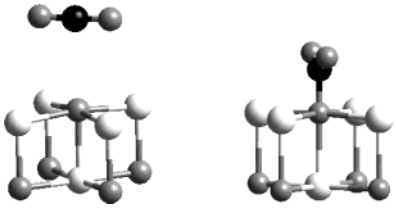

Figure 5. CO_2 adsorption on MgO (left), CaO, SrO, and BaO (right). For clarity, only the cluster without embedding is displayed. The oxygen atoms are given in gray, metal in white, and carbon in black.

TABLE 5: Adsorption Geometry (distances in Å and angles in degrees) and Energies (in kcal/mol) for CO_2 on Alkaline-Earth-Metal Oxides[a]

substrate	$r(CO_2-O\_s)$	$r(CO)$	$\alpha(OCO)$	$q(CO_2)$	E1	E2
MgO	2.94	1.16	177.3	0.00	−3.5	−94.6
CaO	1.49	1.23	134.0	−0.41	−20.8	−84.7
SrO	1.46	1.24	132.0	−0.52	−29.5	−82.1
BaO	1.44	1.24	130.4	−0.52	−37.8	−82.1

[a] O_s denotes the oxygen surface ion. The charge on adsorbed CO_2 (Mulliken population analysis) is given as $q(CO_2)$. E1 denotes the reaction energy for direct adsorption of CO_2 on a surface oxygen site, whereas E2 is the calculated reaction energy for CO oxidation to CO_2 over a surface peroxide.

phase structure (r(CO) = 1.16 Å, α(OCO) = 180.0°); the situation is very analogous to that found for NO_2 on this substrate. In an earlier study by Pacchioni et al.,[12] CO_2 was found to form a surface complex with MgO. This surface complex represented only a local minimum, however, with only a small barrier toward dissociation into MgO and gas-phase CO_2. In the present work, no barrier is obtained and the geometry optimization using this surface complex as a starting geometry results in a physisorbed state for CO_2. This difference is most likely due to the fairly small model (OMg_5) embedded in point charges used by Pacchioni et al. Despite the relatively small model used by Pacchioni et al., the difference in the results is as expected small, since the central oxygen anion was embedded by magnesium cations described fully by quantum mechanical methods. Thus, no artificial polarization toward the unscreened embedding charges is expected.[20]

For CaO−BaO, CO_2 is considerably distorted with the C−O bond distance stretched by up to 0.08 Å and the O−C−O angle reduced down to 130.0°, close to the ideal carbonate angle of 120°. The adsorption energy is steadily increasing in the series MgO < CaO < SrO < BaO. As can be seen from Table 5 the charge donating ability for BaO is about 27% larger than that of CaO. The adsorption energy obtained here for adsorption on the terrace site for CaO is in good agreement with the MP2 level results (20.8 kcal/mol) of Pacchioni et al.[12]

For completeness we have also considered the reaction of CO with peroxide, although the CO content in the exhaust is expected to be low. The computed reaction energies for surface carbonate formation from peroxide species and CO are 99.0, 89.0, 86.4, and 86.4 kcal/mol for MgO, CaO, SrO, and BaO, respectively. It is thus clear that if surface peroxide ions and gas-phase carbon monoxide are present, CO_2 can readily form. As noted earlier, the reaction energies for CO oxidation reflect the relative stabilities of the surface peroxide and the formed carbonate where the overall energy may be decomposed into three contributions: (i) carbon monoxide oxidation to carbon dioxide, (ii) binding energy of the surface peroxide, and (iii) energy for direct adsorption of carbon dioxide on the regular metal oxide surface. Thus, the total reaction energy for oxidation of carbon monoxide also reflects the oxygen affinity of the adsorbate. The energy associated with formation and dissociation of carbon dioxide from a surface carbonate species is intermediate between surface nitrite and nitrate formation. Binding of nitrate to the surface should thus be thermodynamically more stable than that of surface carbonate species. The corresponding formation energy for the carbonate mineral is, however, larger compared to the nitrate mineral.[40] These results thus indicate that if surface carbonate species do form, they can be expected to inhibit, but not irreversibly, the storage capacity on alkaline-earth-metal oxide surfaces.

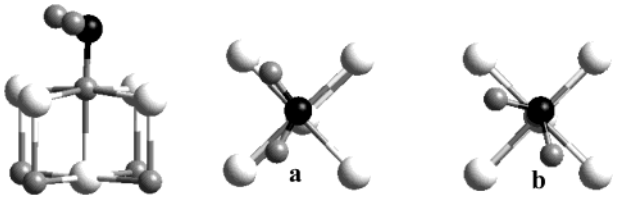

Figure 6. SO_2 adsorption on alkaline-earth oxides. Two different orientations are encountered (a and b). For clarity, only the bare clusters are displayed. The metal atoms are given in white, sulfur in black, and oxygen atoms in gray.

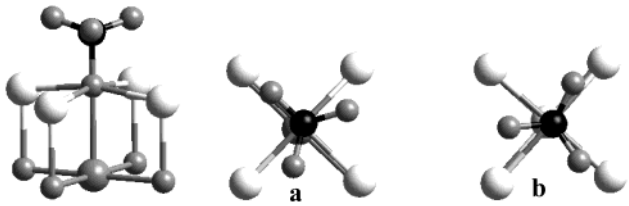

Figure 7. SO_3 adsorption on alkaline-earth oxides. Two different orientations are encountered (a and b), where both give the same adsorption energies for all oxides. For clarity, only the bare clusters are displayed. The metal atoms are given in white, sulfur in black, and oxygen atoms in gray.

TABLE 6: Geometry (distances in Å and angles in degrees) and Adsorption Energies (in kcal/mol) for SO_2 Adsorbed on Alkaline-Earth Oxides[a]

substrate	$r(SO_2-O\_s)$	r(SO)	α(OSO)	$q(SO_2)$	energy
MgO	2.15	1.49	115.2	−0.10	−16.8
CaO	1.94	1.50	113.5	−0.30	−34.1
SrO	1.86	1.51	113.2	−0.37	−41.3
BaO	1.84	1.51	112.0	−0.43	−46.6

[a] O_s denotes the oxygen surface Ion. The charge on adsorbed SO_2 (Mulliken population analysis) is given as $q(SO_2)$.

SO_2 and SO_3 Adsorption. The calculated SO_2 and SO_3 adsorption energies show trends similar to those already found for the previous adsorbates considered. According to the computed adsorption energies, SO_2 is strongly chemisorbed on all the oxides and stable surface sulfite is formed. This is also reflected in the perturbation of the SO_2 internal geometry upon adsorption, where the S−O bond distances become elongated and the O−S−O angle smaller compared to the gas-phase geometry (r(SO) = 1.47 Å, α(OSO) = 117.7°). The orientation relative to the surface changes along the series MgO−BaO (Figure 6). For MgO the oxygens in SO_2 are oriented toward the nearest surface cations (Figure 6a). CaO turns out to represent a transition for the SO_2 orientation on the surface, where oxygen orientation toward the nearest surface cations and the surface oxygen give the same adsorption energy. For SrO and BaO the oxygens in the adsorbed SO_2 are oriented toward the nearest surface oxygens. (See Figure 6b). It is however important to stress that the energy difference between these two orientations is very small (e.g., 0.7 kcal/mol for SrO). For MgO and CaO we obtain the same orientation as in the work by Pacchioni et al.[12] SO_3 is also chemisorbed on all oxides (Figure

TABLE 7: Geometry (distances in Å and angles in degrees) and Adsorption Energies (in kcal/mol) for SO_3 Adsorbed on Alkaline-Earth Oxides[a]

substrate	$r(SO_3-O\_s)$	$r(S-O_a)$	$r(S-O_b)$	$\alpha(O_aSO_a$	$\alpha(O_aSO_b)$	$q(SO_3)$	E1	E2
MgO	1.87	1.48	1.47	117.6	116.7	−0.22	−35.5	−83.4
CaO	1.75	1.48	1.48	116.2	115.4	−0.40	−62.3	−83.5
SrO	1.73	1.48	1.48	115.3	115.1	−0.48	−71.5	−81.4
BaO	1.69	1.50	1.50	113.7	114.9	−0.51	−87.6	−89.2

[a] O_s denotes the oxygen surface ion. The charge on adsorbed SO_3 (Mulliken population analysis) is given as $q(SO_3)$.). E1 denotes the reaction energy for direct adsorption of SO_3 on a surface oxygen site, whereas E2 is the calculated reaction energy for SO_2 oxidation to SO_3 over a surface peroxide site.

7). Here, the orientation of SO_3 changes slightly along the series, where for MgO two of the SO_3 oxygens are oriented toward the nearest cations. For CaO, SrO, and BaO the orientation toward surface cations and surface anions give practically the same adsorption energy. For BaO, these oxygens are slightly rotated (only by a few degrees) away from these surface cations, but the two orientations are basically isoenergetic. The geometry of the adsorbed SO_3 changes upon adsorption with the SO_3 unit becoming more sp^3 hybridized. The S−O bond distances increase for adsorption on all oxides and the O−S−O angle becomes smaller compared to the gas-phase structure (r(SO) = 1.45 Å, α(OSO) = 120.0°). Again, the population analysis shows an increased charge donation from the substrate to the adsorbate along the series MgO−BaO for both SO_2 and SO_3 adsorption (see Tables 6 and 7). The charge donation from the BaO substrate to the SO_2 and SO_3 adsorbates is, respectively, more than four and two times higher than for chemisorption on MgO.

The reaction leading to sulfate formation from SO_2 and a surface peroxide ion is strongly exothermic for all substrates. Here the reaction energy is substantially higher (83.4, 83.5, 81.4, and 89.2 kcal/mol for MgO, CaO, SrO, and BaO, respectively) compared to direct formation of sulfate from SO_3 and a surface anion. These energies are somewhat lower for MgO, CaO, and SrO compared to carbonate formation over surface peroxide. This is a result of the fact that the oxygen affinity (or OC−O binding energy) is substantially larger (125.7 kcal/mol)[41] compared to that of sulfur dioxide (83 kcal/mol).[42] In all cases, the energies related to formation of both sulfite and sulfate species are considerably higher compared to nitrite and nitrate formation. This means that thermodynamically both SO_2 and SO_3 will strongly and, under the relevant conditions, irreversibly inhibit NO_x storage on alkaline-earth oxides.

Summary and Conclusions

The present investigation reveals that essentially the same bonding mechanisms exist for all the species on all the substrates. The exception to this is the MgO substrate for which the small lattice parameter results in a stabilization of the anions that is sufficient to minimize the charge transfer from the surface to the adsorbate that constitutes an important contribution to the bonding interaction. For CaO, SrO, and BaO the bonding modes are qualitatively similar, but differ in the degree of charge transfer that occurs. Several different possible adsorption sites exist for both NO_2 and NO_3 adsorption; the most stable is found to correspond to a cation-pair site in agreement with what was found for MgO by Schneider et al. Reaction with peroxo to oxidize NO to NO_2 or NO_2 to NO_3 is found to be strongly exothermic in all cases. The ability of BaO to easily form peroxo species from, e.g., gas-phase molecular O_2, could thus be a key point to understanding the specific efficiency of this substrate for NO_x storage. It should be noted, however, that NO_x storage occurs also in an oxygen-depleted atmosphere, albeit with lower efficiency. Furthermore, under more realistic conditions, i.e., in an atmosphere containing, e.g., water, $Ba(OH)_2$ will most likely form which should influence the NO_x storage process. However, if peroxide is present at the surface then it should lead to the enhanced NO_x storage observed experimentally as well as deduced in the present work. In this context we note that BaO_2 and SrO_2 are both stable at room temperature, while MgO_2 and CaO_2 are unstable and cannot be prepared without significant water and/or hydrogen peroxide.[33] The specific aspects of the BaO substrate that lead to this particular substrate presently being considered for NO_x storage become of particular interest in view of the similar bonding mechanisms that have been found for all substrates in the present study. These aspects are under investigation and will be the subject of a forthcoming study.[14]

The results from this work indicate that if surface carbonate species do form, they can be expected to inhibit, but not irreversibly, the storage capacity on alkaline-earth-metal oxide surfaces.

For all substrates, the energies related to formation of both sulfite and sulfate species are considerably higher compared to nitrite and nitrate formation. This means that thermodynamically, both SO_2 and SO_3 will strongly and, under the relevant conditions, irreversibly inhibit NO_x storage on alkaline-earth oxides.

Acknowledgment. All the calculations were performed on the Origin3000/3800 located at NTNU in Trondheim. The computer facility at NTNU is organized under the NOTUR program, which is partly funded by the Norwegian Research Council. A generous grant of CPU-time is hereby acknowledged. We thank the staff at NTNU for the technical support.

References and Notes

(1) Taylor, K. C. *Catal. Rev., Sci. Eng.* **1993**, *45*, 467.
(2) Matsumoto, S. *Catal. Today* **1996**, *29*, 43.
(3) Broqvist, P.; Panas, I.; Fridell, E.; Persson, H. *J. Phys. Chem. B* **2002**, *106*, 137.
(4) Fridell, E.; Persson, H.; Westerberg, B.; Olsson, L.; Skoglundh, M. *Catal. Lett.* **2000**, *66*, 71.
(5) Hess, C.; Lunsford, J. H. *J. Phys. Chem. B* **2002**, *106*, 6358.
(6) Schneider, W. F.; Hass, K. C.; Miletic, M.; Gland, J. L. *J. Phys. Chem. B* **2002**, *106*, 7405.
(7) Wyckoff, R. W. G. *Crystal Structures*, 2nd ed.; Wiley: New York, 1963; Vol. 1.
(8) Fridell, E.; Skoglundh, M.; Westerberg, B.; Johansson, S.; Smedler, G. *J. Catal.* **1999**, *183*, 196.
(9) Balcon, S.; Potvin, C.; Salin, L.; Tempere, J.-F.; Djega-Mariadassou, G. *Catal. Lett.* **1999**, *60*, 39.
(10) Rodrigues, F.; Juste, L.; Potvin, C.; Tempere, J.-F.; Blanchard, G.; Djega-Mariadassou, G. *Catal. Lett.* **2001**, *72*, 59.
(11) Schneider, W. F.; Li, J.; Hass, K. C. *J. Phys. Chem. B* **2001**, *105*, 6972.
(12) Pacchioni, G.; Ricart, J.; Illas, F. *J. Am. Chem. Soc.* **1994**, *116*, 10152.
(13) Pyung-Hyun, H.; Yong-Kul, L.; Sang-Min, H.; Hyun-Ku, R. *Top. Catal.* **2001**, *16−17*, 165.
(14) Karlsen, E.; Nygren, M.; Campbell, C.; Pettersson, L. G. M. To be published.

(15) Nygren, M.; Pettersson, L. G. M. *Chem. Phys. Lett.* **1994**, *230*, 456.
(16) Karlsen, E. J.; Nygren, M. A.; Pettersson, L. G. M. *J. Phys. Chem. A* **2002**, *106*, 7868.
(17) Snis, A.; Miettinen, H. *J. Phys. Chem. B* **1998**, *102*, 2555.
(18) Dunning, T. H., Jr. *J. Chem. Phys.* **1970**, *53*, 2823.
(19) Dunning, T. H., Jr.; Hay, P. J. In *Modern Theoretical Chemistry*; Schaefer, H. F., III, Ed.; Plenum: New York, 1976; Vol. 3, p 1.
(20) Nygren, M. A.; Pettersson, L. G. M.; Barandiara'n, Z.; Seijo, L. *J. Chem. Phys.* **1994**, *100*, 2010.
(21) Tatewaki, H.; Huzinaga, S. *J. Comput. Chem.* **1980**, *1*, 205.
(22) Hay, P. J.; Wadt, W. R. *J. Chem. Phys.* **1985**, *82*, 299.
(23) Barandiara'n, Z.; Seijo, L. *J. Chem. Phys.* **1988**, *89*, 5739.
(24) Barandiara'n, Z.; Seijo, L. In *Computational Chemistry: Structure, Interactions and Reactivity*; Fraga, S., Ed.; Elsevier: Amsterdam, 1992; Vol. 77(B).
(25) Ewald, P. P. *Ann. Phys.* **1921**, *64*, 253.
(26) Parry, D. E. *Surf. Sci.* **1975**, *49*, 433.
(27) Parry, D. E. *Surf. Sci.* **1976**, *54*, 195.
(28) Pettersson, L. G. M.; Seijo, L.; Nygren, M. A. *ECPAIMP: an integral program for ECP and AIMP calculations*.
(29) Nygren, M. A.; Hall, R. J. ECPAIMP interface to Gaussian94/98, 1999. The extra links may be obtained by request from L. G. M. Pettersson.
(30) Gaussian 98, A9 ed.; Gaussian Inc.: Pittsburgh, PA, 1998.
(31) Ervin, K. M.; Ho, J.; Lineberger, W. C. *J. Phys. Chem.* **1988**, *92*, 5405.
(32) Olsson, L.; Persson, H.; Fridell, E.; Skoglundh, M.; Andersson, B. *J. Phys. Chem. B* **2001**, *105*, 6895.
(33) Königstein, M.; Catlow, C. R. A. *J. Solid State Chem.* **1998**, *140*, 103.
(34) Chase, M. W., Jr. *NIST-JANAF Thermochemical Tables*, 4th ed.; *J. Phys. Chem. Ref. Data, Monograph 9*, **1998**.
(35) Davidson, J. A.; Fehsenfeld, F. C.; Howard, C. J. *Int. J. Chem. Kinet.* **1977**, *9*, 17.
(36) Karlsen, E. J.; Pettersson, L. G. M. *J. Phys. Chem. B* **2002**, *106*, 5719.
(37) Mestl, G.; Rosynek, P.; Lunsford, J. H. *J. Phys. Chem. B* **1998**, *102*, 154.
(38) Mestl, G.; Rosynek, P.; Lunsford, J. H. *J. Phys. Chem. B* **1997**, *101*, 9321.
(39) Karlsen, E. J.; Nygren, M. A.; Pettersson, L. G. M. To be published.
(40) *CRC Handbook of Chemistry and Physics 2002*−*2003*, 83rd ed.; CRC Press: Boca Raton, FL, 2002.
(41) Curtiss, L. A.; Raghavachari, G. W.; Trucks, G. W.; Pople, J. A. *J. Chem. Phys.* **1991**, *94*, 7221.
(42) Sellers, H.; Shustorovich, E. *Surf. Sci.* **1996**, *356*, 209.